



5th International Conference of Materials Processing and Characterization (ICMPC 2016)

## Effect of self- assembled ZnO<sub>2</sub> intermediate layer on the growth of starch capped ZnO/ ZnS core/shell nano composites through chemical bath deposition method

Sujata Deb <sup>a\*</sup>, P.K. Kalita <sup>b</sup> and P. Datta <sup>c</sup>

<sup>a, c</sup> Department Of ECT, Gauhati University, Guwahati-781014, Assam, India

<sup>b</sup> Department Of Physics, RGU, Rono Hills Doimukh-791112, Arunachal Pradesh, India

### Abstract

ZnO and ZnO/ZnS are simultaneously synthesized through green synthesis route. It has been perceived that reaction time has a great influence on the formation of metal oxides. Thus, the relation between the reaction time and their formation mechanism is discussed here. HRTEM morphology shows the formation of self-assembled intermediate ZnO<sub>2</sub> layer over the core ZnO and thereby it exhibits (ZnO/ZnO<sub>2</sub>)/ZnS composite nanostructure. The broaden peaks of XRD suggests the formation of nanosize core/shell, which agrees well with the HRTEM images. The UV-vis absorption shows strong blue-shift. The corresponding Tauc's plot reveals the possible band gap of ZnO and ZnO<sub>2</sub> as 4.4 eV and 5.4 eV respectively. PL spectroscopy shows a clear emission peaks around 390 nm and 480 nm for double layered core (ZnO/ZnO<sub>2</sub>) as well as for core shell composite [(ZnO/ZnO<sub>2</sub>)/ZnS]. However, the PL intensity decreases for the core/shell structures which may be attributed to the ZnO<sub>2</sub> layer. ZnO<sub>2</sub> acts as potential gradient at the interface and facilitates charge separation which in turn reduces recombination between the excited holes and electrons. Thus, ZnO<sub>2</sub> layer can have a potential to enhance the photo-conversion efficiency in ZnO nanocomposites.

©2017 Published by Elsevier Ltd.

Selection and peer-review under responsibility of Conference Committee Members of 5th International Conference of Materials Processing and Characterization (ICMPC 2016).

*Keywords:* core/shell; ZnO/ZnO<sub>2</sub>/ZnS; HRTEM; Photoluminescence; reaction time.

\* Corresponding author. Tel.: +0-986-420-0175

E-mail address: [sujatabmk@gmail.com](mailto:sujatabmk@gmail.com)

## 1. Introduction

Core/Shell nanostructures have engrossed much interest because of their most intriguing varied applications that can be engineered to enhance the unique properties of the nanostructures. There are more than a few other ways to synthesize core/shell nanostructures, but the method used here is economically feasible and moves towards a facile, non-toxic and low-temperature heat treatment route. Adding a shell to the core provides a way to control the functionality of these structures, which can be used to emit light for biomedical imaging, LEDs and spectroscopy or photocurrents for solar cells and chemical sensors [1-5]. Zinc oxide (ZnO) is the only semiconductor material extensively investigated after Si/Ge. It belongs to II-VI group semiconductors class and has a wide direct band gap between 3.1 and 3.37 eV at room temperature and has a large binding energy (60 meV). It has gained a tremendous amount of theoretical and experimental interests due to its unique nanoscale range of technological applications [6-8]. Encapsulation of a semiconductor with another semiconductor of wide band gap has been recognized as one of the highly developed methods to enhance the optical properties [9]. Zinc sulfide (ZnS) is one such most important shell materials used for over coating numerous II-VI and III-V semiconductor nanostructures to enhance their luminescent property. It is a wider band gap (3.7 eV at room temperature) semiconductor material and has large exciton binding energies of 40 meV, having noticeable applications [10]. Besides, both the materials are abundant, extremely stable, and biologically friendly. Scientists around the world have performed very extensive and promising work in this field. But it is furthermore feasible to engineering new materials to this arena. In this paper, we report the impact of reaction time on the morphology and luminescence characteristics of the nanostructures. It has been perceived from high resolution transmission electron microscopy (HRTEM) morphology, the formation of self-assembled intermediate  $ZnO_2$  layer over the ZnO consequently exhibiting ZnO/ $ZnO_2$ /ZnS composite nanostructure.  $ZnO_2$  material is an indirect semiconductor with a wide energy gap of about 4.5 eV. It is reported by other workers that it gets decomposed under constant heating to release oxygen [11]. For a better understanding of the relation between the morphology and reaction time, sample with longer duration reaction time has also been synthesized. By increasing reaction time, HRTEM study evidences the formation of single layered core ZnO, presenting ZnO/ZnS composite nanostructure, with enhancement of the photoluminescence (PL) property. Thus,  $ZnO_2$  facilitates charge separation reducing recombination between the excited holes and electrons. Hence,  $ZnO_2$  layer can have a potential to heighten the photo-conversion efficiency in ZnO nanocomposites.

### 2.1 Experimental Details

All analytic grade reagents of Merck are used as received without any alteration. Two samples of core shell ZnO/ZnS with same volume metric ratio (1:1.5) via chemical bath deposition method (CBD) are prepared through green synthesis route at a temperature as low as 90 °C. The preparation technique consisted of two stages-(i) the growth of core (ZnO) nanostructures and then (ii) the development of a shell (ZnS) to encapsulate the core. Zinc acetate [ $Zn(CH_3COO)_2 \cdot 2H_2O$ ], sodium hydroxide (NaOH), thiourea ( $NH_2CS.NH_2$ ) and ammonia are selected as raw materials to synthesize ZnO/ZnS core/shell nanostructures. In the first approach, the growth time of core (ZnO) nanostructure is considered shorter (sample-1 for 1.5 hrs.). In order to discuss the influence of reaction time, second approach is considered keeping the duration of reaction time longer for core formation (sample-2 for 3.5 hrs.), with both the samples being heated in air at same temperatures (90 °C). The formation of  $ZnO_2$  in case of sample-1 can be understood as it is readily formed from the oxidation of zinc acetate with sodium hydroxide at a shorter duration of reaction. With increase of duration of reaction time during the core synthesis,  $ZnO_2$  is observed to get transformed to ZnO; it gets decomposed by constant heating for longer growth time at 90 °C to release oxygen. Thereafter core formation, the ZnO/ZnS core/shell nanostructures are synthesized under nitrogen environment with respect to same volume ratio (1:1.5) of core and shell matrix solution. During the shell formation, ZnO may have reacted with sulphide ions released from an equimolar (0.5M) solution of  $NH_2CS.NH_2$  and gets converted into ZnS over ZnO core. In the synthesis process, starch is used as a capping agent and ammonia as a complexing agent for preparation at alkaline medium, adjusting the pH of the solution at  $\approx 11$ . The whole of the synthesis process is carried out in distilled water for being environmentally benign. Prior to use, ordinary glass substrates are thoroughly rinsed in ethanol and de-ionized water. The cleaned glass substrates are then dipped into the resultant matrix solutions to obtain all the sample thin films for XRD studies. The samples are also arranged as colloidal solutions for optical as

well as HRTEM studies. The as-prepared samples films are finally stored in airtight desiccators at room temperature for all characteristic studies.

## 2.2 Characterization

All the as-prepared products have been characterized by standard techniques via – high resolution transmission electron microscopy (HRTEM), UV-Vis and photoluminescence (PL) spectroscopy. The Phase purity and crystalline size of the as-prepared products are determined by an X-ray diffractometer (Seifert 3003-TT), using Cu-K $\alpha$  radiation. The sample -1, XRD data is collected over an angular range of  $30^\circ < 2\theta < 70^\circ$  in step scan mode with step 0.03 using Cu-K $\alpha$  radiation ( $\lambda = 0.15406$  nm) while via same radiation and wavelength, XRD data of sample -2, is collected over an angular range of  $15^\circ < 2\theta < 75^\circ$  in continuous scan mode with step 0.05. Morphological study of each sample are recorded on a high resolution transmission electron microscope (JEOL JEM-2100) operated at voltage 200 KV. Selected area electron diffraction (SAED) patterns are also developed with prominently observed d-values while HRTEM measurements are done. Optical absorption measurements are recorded using UV-visible spectrophotometer (a model-UV-1800), Shimadzu in the range 150 nm to 700nm. The photoluminescence (PL) measurements of the samples are recorded using a Hitachi FL spectrophotometer (model-F-2500) with excitation wavelength of 260 nm having scan speed as 500 nm/min.

## 3 Results and discussion

The XRD analysis indicates that the films are polycrystalline. Figure 1 showing X-ray diffraction (XRD) pattern of sample-1 unveils that in addition to ZnO peaks, the ZnO<sub>2</sub> peaks are also obtained with shorter duration (1.5 hrs. ) of reaction time. Conversely, with increasing reaction time (sample-2), ZnO peaks gradually dominate at a cost of drop of ZnO<sub>2</sub> peaks. The main dominant broad peaks for ZnO are identified at  $2\theta = 31.79^\circ, 34.43^\circ, 36.7^\circ, 47.8^\circ, 56.78^\circ$  and  $63.28^\circ$ , which correspond to indexes (100), (002), (101), (102), (110) and (103), respectively that indicate typical hexagonal wurtzite type structure of ZnO nanostructures. The observed diffraction planes are in good agreement with JCPDS file no. 36-1451. However, as-prepared sample shows various diffraction peaks at  $2\theta = 33.08^\circ$  (111),  $36.38^\circ$  (200),  $41.63^\circ$  (210),  $44.8^\circ$  (211),  $53.38^\circ$  (220), and  $63.02^\circ$  (311) that can be indexed to the crystalline structure of the zinc peroxide (ZnO<sub>2</sub>) nanoparticles which confirms the formation of intermediate self-assembled shell ZnO<sub>2</sub>, exhibiting ZnO/ZnO<sub>2</sub> doubled layer core composite nanostructure. The planes of ZnO<sub>2</sub> are in well agreement with standard literature. Possible existence of ZnO<sub>2</sub> is explained by other workers under varied reaction conditions, depending on growth parameters, such as synthesis temperature and duration of reaction [12]. The as-prepared sample also shows various diffraction peaks at  $30.65^\circ$  (101),  $39.17^\circ$  (102),  $49.03^\circ$  (220),  $57.0^\circ$  (311) and  $59.01^\circ$  (004) corresponding to the cubic ZnS blende. The diffraction peaks of face centred cubic zinc blende structure with lattice constants  $a = 5.406$  Å are in good agreement with the values in the standard card (JCPDS file 05-0566). And some unknown peaks can be identified as zinc hydroxide peaks; however with longer duration, zinc hydroxide conversion takes place. The lattice parameters of the hexagonal wurtzite ZnO are calculated corresponding to most prominent peaks of ZnO which are found to be  $a = 3.249$  Å and  $c = 5.2393$  Å that are in good agreement with standard literature. The average particle size,  $D_{\text{of ZnO}}$  calculated by using well known Scherrer formula is found to be 8.51 nm and 9.69 nm for sample-1 and sample-2 respectively, which are in fair agreement with sizes estimated from respective HRTEM studies.

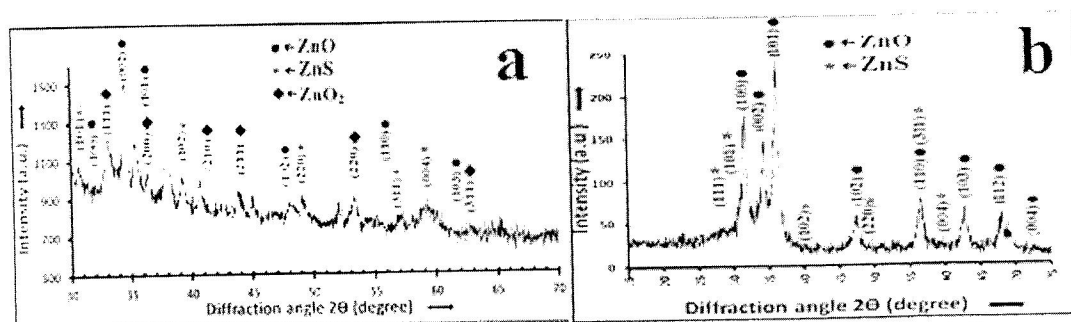


Fig. 1 XRD pattern of starch capped (a) sample-1 (ZnO/ZnO<sub>2</sub>)/ (ZnS) (b) sample-2 (ZnO/ZnS) core-shell nanostructures

To study the structural and morphological data in details, HRTEM is conducted. Among many experimental parameters, for instance, pH of solution, reaction time and temperature, the reaction time plays a substantial role in the formation of metal oxides. Figure 2 and figure 3 show HRTEM images of sample-1 and sample-2 under different reaction time: (a) 1.5 hrs and (b) 3.5 hrs respectively. ZnO crystals being divalent metal ions, do not hydrolyse in acidic environments, as such an alkaline solution is essential for the formation of ZnO nanostructures. ZnO is seen to crystallize by the hydrolysis of Zn salts i.e., Zinc acetate  $[\text{Zn}(\text{CH}_3\text{COO})_2 \cdot 2\text{H}_2\text{O}]$  in a basic solution that is formed using alkali compound, NaOH. The reaction between sodium hydroxide and zinc acetate leads to the formation of zinc hydroxide,  $\text{Zn}(\text{OH})_2$ , which then decomposes under constant heating process. The product could also be in the form of  $\text{Zn}(\text{OH})_4^{2-}$  or  $\text{Zn}(\text{OH})^+$ , depending on parameters such as the concentration of  $\text{Zn}^{2+}$  and the pH value, which has been observed by other workers as well [12]. All of these intermediate products are in equilibrium, with the dominant products being different under different reaction conditions. And different types of inherent composites have already been reported like Zn–ZnO core–shell, ZnO/Zn(OH)<sub>2</sub> and Zn(OH)<sub>2</sub>/ZnO<sub>2</sub> [13–14]. Subject to the given growth parameters a series of intermediates could exist and ZnO can be formed by the dehydration of these intermediates. Therefore a detailed study on growth parameters is still desirable. T.Thi Ha et al. [15] suggested that the growth of ZnO nanocomposites is sensitive to the reaction time, and their morphologies can be tuned and controlled by adjusting growth parameters. HRTEM morphology of sample-1 shows the formation of self-assembled intermediate ZnO<sub>2</sub> layer over the ZnO, thereby exhibiting (ZnO/ZnO<sub>2</sub>)/ZnS composite nanostructure. On the other hand, HRTEM investigation of sample-2, support for the formation of single layered core ZnO and shell ZnS exhibiting ZnO/ZnS core/shell composite nanostructures. The HRTEM image of as-prepared ZnO/ZnS nanostructure shows a sharp contrast between ZnO and ZnO<sub>2</sub> nanostructures [Fig. 2(b)]. The images (2c) clearly shows the d-parameter 0.26 nm corresponds to (002) planes of ZnO. The SAED pattern of ZnO/ZnS core/shell structures shown inset of the Figure-3 shows spotted pattern and a set of concentric ring diffraction pattern. The spots correspond to diffraction of polycrystalline ZnO. The rings are diffraction of ZnS nanocomposites [16]. And fig. 3(c) shows the HRTEM image of sample-2 ZnO/ ZnS displaying the average size of core/shell nanocomposites.

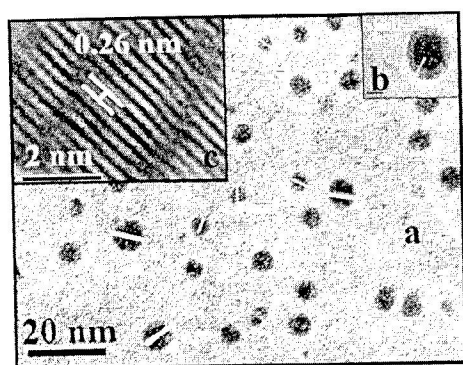


Fig. 2 HRTEM images of (a) ZnO/ZnO<sub>2</sub> nanocomposite, (b) inset shows its magnified form and (c) observed d-values of ZnO.

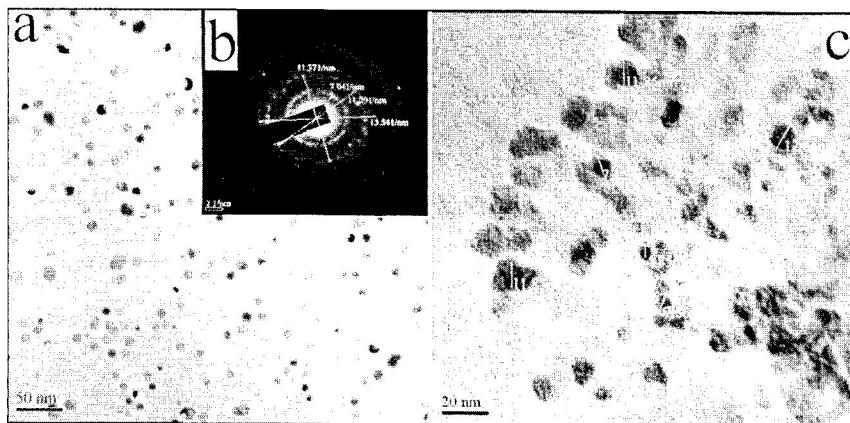


Fig. 3 HRTEM images (a) of sample-1 (ZnO/ZnO<sub>2</sub>/ZnS core/shell) showing its average size, (b) inset shows its SAED pattern, (c) HRTEM image of sample-2 (ZnO/ ZnS) displaying its average size

Figure- 4(a) shows Tauc's plot of sample-1 nanocomposites. The sample-1 indicates prominent excitonic absorption peaks at around 219, 280 nm and 300 nm. The excitonic absorption lies below the band gap wavelength of bulk ZnO (365 nm) [17], demonstrating that the nanocomposite exhibits highly strong blue-shift compared to that of bulk ZnO, owing to the quantum confinement effect. Moreover, since bulk bandgap of ZnO<sub>2</sub> is about 4.5 eV, it is expected to enhance 5.4 eV as from Tauc's plot. The band gap energy of the as-prepared nanoparticles is evaluated from the UV-Vis spectra by using the Tauc relation,

$$(\alpha hv) = c(hv - E_g)^n \quad (1)$$

where  $\alpha$  is the absorption coefficient  $c$  is a constant,  $E_g$  is the band gap, and  $n = \frac{1}{2}$  for direct band gap semiconductor. The value of band gap is estimated from an extrapolation of the plot of  $(\alpha hv)^2$  versus the incident photon energy  $hv$ .

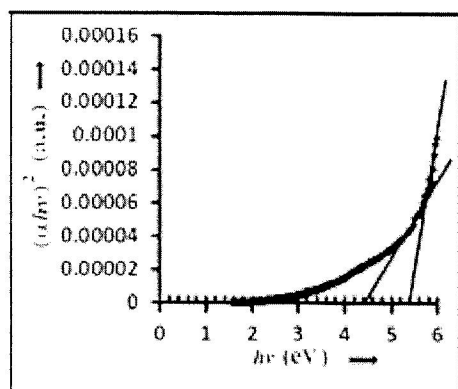


Fig.4 Tauc's plot of core (ZnO/ZnO<sub>2</sub>) of sample-1 nanocomposites.

The photoluminescence spectra of core-shell nanostructures (sample-1 and sample -2) embedded in starch matrix have been depicted in Fig. 5. PL spectrum shows near band gap emission at 390nm in the UV region and 395 nm of sample-1 and sample - 2 respectively and extrinsic emissions at around 480 nm(sample-1) and 450 nm and 464nm(sample-2). The observed near band gap photoluminescence may be attributed to the radiative recombination process of electrons and holes confined in nanoparticles, whereas extrinsic emission is overseen by surface defects. However, the PL intensity in case of sample-1, decreases for the core/shell structures. The reduction in the

PL intensity may be recognized to the  $\text{ZnO}_2$  intermediate self-assembled shell, which plays an important role in enhancing the arrival flux of charge carrier to the ZnO surface.  $\text{ZnO}_2$  results in a potential gradient at the interface because of the variance in band structure between ZnO and  $\text{ZnO}_2$ . This potential gradient facilitates charge separation and hence reduces recombination between the excited holes and electrons. In addition, the other structural surface states created near ZnO/ $\text{ZnO}_2$  interfaces also serve as favourable trap sites for excitons to reduce their recombination. And hence the PL intensity found to decrease for the core/shell structures. However, with increase of reaction time during core synthesis,  $\text{ZnO}_2$  is observed to get transformed to ZnO and the PL intensity of (ZnO)/ZnS core/shell nanocomposites is found to get enhanced on coating ZnO with ZnS at a cost of decrease of  $\text{ZnO}_2$  layer. P. K. Giri *et al.* [18] also reported that the ZnO/ $\text{ZnO}_2$  core-shell structure is obtained with shorter reaction time and  $\text{ZnO}_2$  later converts to ZnO for longer duration reaction. Hence, though PL decreases with short reaction time, the intensity again seen to increase on shell (ZnS) formation with longer reaction time. Thus, our results indicate that a higher reaction time enhanced the PL intensity of the core/shell nanocomposites. Further, it shows that shell growth goes together with by a small red shift of the excitonic peak in the photoluminescence (PL) wavelength pertaining to bare core ZnO. This observation can be recognized to a partial leakage of the exciton into the shell material. Earlier report also evidenced the red shift of core/shell nanostructure over the core [19].

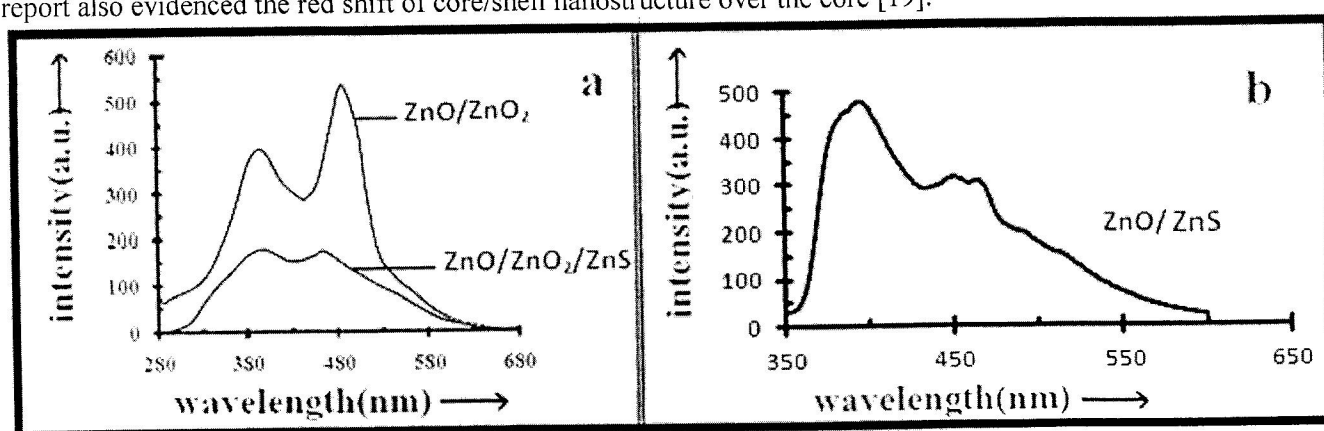


Fig.5 PL emission spectra of (a) sample-1( ZnO/ZnO<sub>2</sub> and ZnO/ZnO<sub>2</sub>/ZnS) (b) sample-2( ZnO/ZnS) nanocomposites

### 3.1 Conclusion

ZnO and ZnO/ZnS are simultaneously synthesized via chemical bath deposition method through green synthesis route at a low temperature as  $90^\circ\text{C}$ . The success of the work reported in this paper is that a cost-effective method has been demonstrated to synthesis core/shell structures and moreover it is developed that reaction time has a great effect on the formation of metal oxides. Thus, a wide-ranging method is demonstrated to produce functional semiconductor core/shell with a variety of compositions and forms for unique properties. The morphology, band gap and other optical properties of the as-synthesized ZnO along with their core/shell structures have been characterized by standard techniques. The XRD shows the presence of both hexagonal ZnO and cubic ZnS in core / shell nanostructure. HRTEM morphology (sample-1) shows the formation of self-assembled intermediate  $\text{ZnO}_2$  layer over the ZnO and thereby it exhibits double layered core (ZnO/ $\text{ZnO}_2$ )/ shell (ZnS) composite nanostructure. The UV-vis absorption spectrum shows an absorption edge around 280 nm, which shows the quantum confinement because of blue-shift. PL spectroscopy shows a clear emission peaks around 390 nm and 480 nm for core ZnO/ $\text{ZnO}_2$  as well as for core/shell composite ZnO/ $\text{ZnO}_2$ /ZnS. However, the PL intensity decreases for the core/shell structures. This may be attributed to the  $\text{ZnO}_2$  intermediate self-assembled shell, which plays an important role in enhancing the arrival flux of charge carrier to the ZnO surface. However, it is observed that with longer core formation time growth (sample-2) the photoluminescence (PL) property of ZnO/ZnS core/shell nanostructures can be greatly enhanced. Thus,  $\text{ZnO}_2$  facilitates charge separation, indicating that  $\text{ZnO}_2$  layer can have a potential to intensify the

photo-conversion efficiency in ZnO nanocomposites. Therefore, the chemical growth of ZnO and ZnO/ZnS nanostructures and the characterization results of the grown samples corresponding to modulation of optical properties have been reported. Henceforth the fabrication of core/shell nanostructures through appropriate growth time will bring in possibilities for a wide range of application fields.

### Acknowledgements

Authors gratefully acknowledge the technical support of the Department of Physics, Guwahati College, Guwahati, Department of Physics and Centre for Nanotechnology, IIT-Guwahati for XRD analysis, Department of Chemistry, Gauhati University for UV-Visible and PL measurements and the Sophisticated Analytic Instrument Facility (North Eastern Hill University) Shillong for HRTEM studies.

### References

- [1] H. Kim et al. Characteristics of CuInS<sub>2</sub>/ZnS quantum dots and its application on LED. *J. Cryst. Growth* 2011; 326: 90-93.
- [2] M. C. Newton and R. Shaikhaidarov. *Appl. Phys. Lett.* 2009; 94: 153112-3.
- [3] M. Bruchez Jr., M. Moronne, P. Gin, S. Weiss, A. Paul Alivisatos. *Science* 1998; 281: 2013-2016.
- [4] G. Morello et al. *Nanoscale Res. Lett.* 2007; 2: 512-514.
- [5] J. Sun, J. Zhuang, S. Guan, W. Yang. *J. Nanopart. Res.* 2008; 10: 653-658.
- [6] R. Chakraborty, U. Das, D. Mohanta and A. Choudhury. *Indian Journal of Physics* 2009; 83: 553-558.
- [7] C. A. Mirkin. *Science* 1999; 286: 2095-2096.
- [8] J. Sudeepan, K. Kumar, T. K. Barman, P. Sahoo. *Advanced Materials Manufacturing & Characterization* 2015; 5: 125-135.
- [9] J. Li et al. *J. Phys. Chem. B* 2006; 110: 14685-7.
- [10] P. Verma, A. C. Pandey, Controlled Growth of CdS Nanocrystals: Core/Shell viz Matrix. *J. Biomater Nanobiotechnol* 2011; 2: 409-413.
- [11] K. A. Kim et al. *Bull. Korean Chem. Soc.* 2014; 35: 431-435.
- [12] M. Hasanpoor, M. Aliofkhaezrai, H. Delavari. *Procedia Materials Science* 2015; 11: 320-325.
- [13] G. Mu *PhD Thesis* (Missouri University of Science and Technology, China) 2010.
- [14] P. Amornpitoksuk, S. Suwanboon. *Power Technology* 2010; 203: 243-247.
- [15] T. T. Ha, T. D. Canh, and N. V. Tuyen. *ISRN Nanotechnology* 2013; 2013: 497873
- [16] S. K. Panda, A. Dev, and S. Chaudhuri, Fabrication and Luminescent Properties of *c*-Axis Oriented ZnO-ZnS Core-Shell and ZnS Nanorod Arrays by Sulfidation of Aligned ZnO Nanorod Arrays. *J. Phys. Chem. C* 2007; 111: 5039-5043
- [17] C. Jagadish and S. J. Pearton. *Zinc Oxide Bulk, Thin Films and Nanostructures: Processing, Properties, and Applications* (U.K.: Elsevier's Science and Technology) 1; 2006: 6
- [18] P. K. Giri et al. *Journal of Nanoscience and Nanotechnology* 2011; 11: 1-6.
- [19] R. G. Xie, U. Kolb, J. X. Li, T. Basche, A. Mews, Synthesis and characterization of highly luminescent CdSe-Core CdS/ZnO<sub>0.5</sub> CdO<sub>0.5</sub> ZnS multishell nanocrystal. *J. Am. Chem. Soc.* 2005; 127: 7480-7488.